J Geophys (1984) 56:9–19

Journal of Geophysics

# Frequency dependence of $Q$ for seismic body waves in the Earth's mantle

**A. Ulug* and H. Berckhemer**

Institut für Meteorologie und Geophysik, Feldbergstr. 47, 6000 Frankfurt, Federal Republic of Germany

**Abstract.** In this paper an attempt is made to determine the frequency dependence of $Q$ in the Earth's mantle in the frequency range 0.03–1.5 Hz from the spectral ratio of teleseismic $S$- and $P$-waves. Digital broad-band data of 17 earthquakes at $40° < \Delta < 90°$ recorded at the Central Seismological Observatory of the Federal Republic of Germany at Erlangen were analysed. The method implies the following assumptions: frequency independence of the crustal transfer function, proportionality of $Q_P(f)$ and $Q_S(f)$, and proportionality of $P$- and $S$-source spectra. This last and most critical assumption was carefully investigated by kinematic and dynamic source models.

The calculated $\bar{Q}$-spectra for the individual events vary considerably but all have in common a general increasing trend with frequency which can best be represented by a power law $Q \sim f^{\alpha}$ with $0.25 < \alpha < 0.6$. A further increase in slope near 1 Hz suggests an absorption band corner with an upper cut-off relaxation time $\tau_m = 0.33 \pm 0.18$ s. The significance of the $Q$-spectra and their variability is estimated by manipulating semi-synthetic seismograms with different error-producing processes such as length and shape of the time window, superposition of noise, digital filter process and source spectra. It is concluded that none of these processes is able to destroy or to imitate the observed increasing trend of $Q$ with frequency.

The results are compared with those from other seismological investigations and from laboratory experiments on mantle rocks at high temperature and in the seismic frequency band.

**Key words:** Anelastic wave attenuation in the Earth's mantle – Frequency dependence of $Q$ – Spectral ratio method

## 1. Introduction

Amplitude and shape of seismic signals are, to a large extent, influenced by the anelastic attenuation in the earth. This physical property is most conveniently described by the elastic quality factor $Q$. Detailed knowledge of $Q$ in space and frequency is not only required as a crucial correction term for restoring the seismic source function from teleseismic signals or for generating realistic synthetic seismograms, but also provides intrinsic information on physical properties of the material traversed by the seismic waves. Anelasticity in mantle and core is most probably controlled by thermally activated solid state processes and, therefore, highly temperature dependent. Comparison of laboratory experiments, theory and field observations may lead to a better understanding of the physical processes governing anelasticity, and to temperature estimates in the earth.

Until a few years ago $Q$ was generally treated by seismologists as a frequency independent quantity, chiefly because of the lack of more precise information. The constraints to assume some increase of $Q$ with frequency, however, are growing. For the Earth's mantle the number of specific investigations with regard to the frequency dependence of $Q$ is still very limited, e.g. Sipkin and Jordan (1979), Lundquist and Cormier (1980), Der et al. (1982). These and other studies are based on differences in attenuation derived from long- and short-period seismograms, but not from continuous spectra over a broader frequency band. The mode of variation of $Q$ with frequency deduced from these data remains, therefore, ambiguous. Also, depending on the method applied, it is often difficult to separate spatial variations of $Q$ from those in frequency (e.g. Der et al. 1982). This is true, in particular, for all $Q$ determinations from surface waves.

The exclusive aim of the present study is to obtain $Q$-spectra estimates for mantle body waves. No attempt is made to determine absolute values or spatial variations of $Q$. The authors were motivated to this study by laboratory measurements of $Q$ by Berckhemer et al. (1979, 1982 and unpublished results). These experiments, which surpassed the solidus temperature of peridotite and dunite, were considered to be of relevance to the anelasticity of the upper mantle, especially of the asthenosphere. Consequently, the $Q$-structure in the Earth's mantle was also investigated, in particular its possible frequency dependence, and both results compared.

A continuous spectrum of $Q(f)$ can only be determined if attenuation is measured over a sufficiently wide frequency band along a well specified ray path.

* Present address: Dokuzeylül Universität, Institute of Marine Sciences and Technology, P.O. Box 478, Konak-Izmir, Turkey

*Offprint requests to:* H. Berckhemer

This requires knowledge of the seismic signal spectrum at both ends of the path, and of all factors influencing the amplitude spectrum along the path.
Since the frequency dependence of $Q$ can not be expected to be very large it is insufficient to replace the source spectrum just by some simple theoretical model, as done for constant-$Q$ estimates by several authors (e.g. Tsujiura, 1966; Okada et al., 1970; Burdick, 1978). Use of the spectral ratios of multiple $ScS$ (Sipkin and Jordan, 1979) or $ScS/ScP$ (Kanamori, 1967) eliminates, in principle, the problem of the source spectrum. However, these signals are typically of low signal/noise ratio, in particular at short periods, and are affected by the particular conditions of the core-mantle boundary zone (low-$Q$ zone?).

## 2. Principles of the $S/P$ spectral ratio method

In the present study we use the spectral ratio of $S$ and $P$ of a teleseismic event where both phases are recorded at the same station. This has the advantage of almost identical ray paths, high signal to noise ratio and large contrast in attenuation for both wave types. In fact the less attenuated $P$-signal serves as a kind of reference signal for the unknown source time function. The necessary assumptions to be made are stated below and will be subject to a critical discussion in Sect. 3.

To derive the basic equation for the determination of $Q(f)$ it is convenient to describe the transmission of the seismic signal from the source to the receiver in the frequency domain by a chain of linear filters:

$$A(f)=S(f)\,C(f)\,M(f,\Delta)\,\phi(f,R), \tag{1}$$

where $A(f)$ = seismogram spectrum,
$S(f)$ = seismograph transfer function,
$C(f)$ = transfer function of the receiver crust,
$M(f,\Delta)$ = mantle transfer function,
$\Delta$ = epicentral distance,
$\phi(f,R)$ = source spectrum with
$R$ = source radiation characteristic.

All functions may be complex and, with the exception of $S(f)$, depend on the respective wave type. We are particularly interested in the mantle transfer function $M(f,\Delta)$ which consists of the frequency independent geometrical spreading factor $G(\Delta)$ and the frequency dependent anelastic absorption factor $\exp\left[-\int_s \gamma(f,r)\,ds\right]$ along the ray path $s$, where, for a spherically symmetrical earth, the absorption coefficient $\gamma(f,r)$ is a function of the geocentric distance $r$ and the frequency $f$. Since $\gamma$ is related to $Q$ by

$$\gamma(f,r)\approx \pi f/[Q(f,r)\,v(r)], \tag{2}$$

with the propagation velocity $v(r)$ of the wave type considered, we obtain

$$M(f,r)=G(\Delta)\exp\left[-\pi f\int_s \frac{ds}{Q(f,r)\,v(r)}\right]. \tag{3}$$

Replacing the integral in Eq. (3) by the quotient $t^*$ of travel time $t$ and the mean value $\bar{Q}(f)$ along the ray path $s$

$$\int_s \frac{ds}{Q(f,r)\,v(r)}=\frac{t}{\bar{Q}(f)}=t^*, \tag{4}$$

the spectral ratio of $S$- and $P$-wave recorded at the same station by the same instrument may be written according to Eqs. (1), (3) and (4) as

$$\frac{S(f)}{P(f)}=\frac{C_S(f)}{C_P(f)}\cdot\frac{G_S(\Delta)}{G_P(\Delta)}\cdot\exp\left\{\pi f\left[\frac{t_P}{\bar{Q}_P(f)}-\frac{t_S}{\bar{Q}_S(f)}\right]\right\}\frac{\phi_S(f,R_S)}{\phi_P(f,R_P)}. \tag{5}$$

In order to solve Eq. (5) for $\bar{Q}_S(f)$ and $\bar{Q}_P(f)$ we introduce the following approximations and assumptions:

a) Approximative frequency independence of the crustal transfer functions $C_S(f)$ and $C_P(f)$ in the frequency range 0.01–3 Hz

$$C_S(f),\ C_P(f)\approx\text{const.},\ C_S/C_P=n(\approx 1). \tag{5a}$$

b) Approximative equality of the ray divergence factors $G_S(\Delta)$ and $G_P(\Delta)$

$$G_S(\Delta)\approx G_P(\Delta). \tag{5b}$$

c) Approximative proportionality of $\bar{Q}_S(f)$ and $\bar{Q}_P(f)$. With the common assumption that anelasticity is confined to shear deformation,

$$\bar{Q}_P(f)=k\bar{Q}_S(f),\qquad k=\tfrac{3}{4}(v_P^2/v_S^2)\approx\tfrac{3}{4}(t_S^2/t_P^2). \tag{5c}$$

d) Assumption of proportionality of the source spectra $\phi_S$ and $\phi_P$. This is certainly correct for a point source but neglects the rupture propagation process of a source of finite dimensions:

$$\phi_S(f,R_S)/\phi_P(f,R_P)\approx R_S/R_P=g. \tag{5d}$$

Under these conditions Eq. (5) reads

$$\frac{S(f)}{P(f)}=m\exp\left[\pi f\frac{1}{\bar{Q}_S(f)}\left(\frac{t_P}{k}-t_S\right)\right] \tag{6}$$

with $m=ng$. (6a)

Equation (6) may be resolved with respect to $\bar{Q}_S(f)$, and with Eq. (5c) one obtains

$$\bar{Q}_S(f)=\frac{\pi f}{\ln S(f)-\ln P(f)-\ln m}\,\frac{\frac{4}{3}t_P^3-t_S^3}{t_S^2},$$

$$\bar{Q}_P(f)=\frac{3}{4}\frac{t_S^2}{t_P^2}\bar{Q}_S(f). \tag{7}$$

All quantities in Eq. (7), except the factor $m$, can be directly determined from the seismogram if the travel times are known. The direct determination of the factor $m$, which reflects essentially the ratio of the $S$- and $P$-radiation patterns in the direction of the ray from the source to the station, would require a very accurate and stable fault-plane solution for the event. This can be circumvented by an empirical determination of $m$ using a standard value of $\bar{Q}_S$ (or $\bar{Q}_P$) at a reference

frequency $f_r$. As pointed out already, we are only concerned with the frequency dependence of $Q$, not with its absolute level. Standard values of $t^*(\Delta)=\frac{t(\Delta)}{Q(\Delta)}$ are available from several $Q_P$- and $Q_S$-models. We have chosen $t^*$ values from model SL1 (Anderson and Hart, 1978) and assigned them to a reference frequency $f_r = 0.1$ Hz, typical for the range at which SL1 was determined. Any other reasonable model would do it as well and simply shift the level of $Q(f)$ somewhat, without a significant influence on the frequency dependence of $Q$. From Eq. (7) it follows

$$\ln m = \ln\left[\frac{S(f)}{P(f)}\right] - \pi 0.1 t_S^*(\Delta)\frac{\frac{4}{3}t_P^3 - t_S^3}{t_S^3}, \tag{8}$$

$f = 0.1$ Hz

## 3. Discussion on the assumptions involved

*Crustal transfer function*

The layered structure of the receiver crust acts as a seismic frequency filter. The ratio of surface motion and wave motion at the base of the crust, the crustal transfer function, has been calculated for many crustal structures and angles of incidence $i$ by various authors. Kanamori (1967) has shown that, e.g. for a 4-layer crust and steep incidence ($i = 10°$–$20°$), the ratio of the vertical surface motion and $P$-wave amplitude in the frequency range 0–1 Hz assumes an almost constant average level of 2.5 with variations of $\pm 20\%$, and similar for the ratio of the horizontal ground motion and $SV$ amplitude. Leblanc (1967) has shown that the average of 20 transfer functions of different crustal models varies in the range $0.4 < f < 1.6$ Hz by less than $\pm 1$ dB about a frequency independent mean value. This is considered a sufficient justification to approximate $C_S$ and $C_P$ by frequency independent mean values which do not have to be known explicitly if $m$ is determined empirically.

*Ray divergence factor*

Since the ray divergence at a given epicentral distance is almost identical for $P$- and $S$-waves (e.g. Shimshoni and Ben Menahem, 1970), the ratio of both can safely be assumed to be unity. In any case ray divergence would not affect the frequency dependence of $Q$.

*Relation between $Q_S$ and $Q_P$*

An isotropic solid having anelastic properties can conveniently be described by complex elastic moduli

$$M(f) = M'(f) + iM''(f). \tag{9}$$

Then, the corresponding elastic quality factor is defined as

$$Q(f) = M'(f)/M''(f). \tag{10}$$

The moduli governing the $S$- and $P$-wave propagation, respectively, are

$$M_S(f) = \mu'(f) + i\mu''(f), \tag{11a}$$

$$M_P(f) = K'(f) + \tfrac{4}{3}\mu'(f) + i[K''(f) + \tfrac{4}{3}\mu''(f)], \tag{11b}$$

and the corresponding $Q$-factors

$$Q_S(f) = \frac{\mu'(f)}{\mu''(f)}, \tag{12a}$$

$$Q_P(f) = \frac{K'(f) + \frac{4}{3}\mu'(f)}{K''(f) + \frac{4}{3}\mu''(f)}, \tag{12b}$$

or

$$\frac{Q_S(f)}{Q_P(f)} \approx \frac{v_S^2}{v_P^2}[\tfrac{4}{3} + K''(f)/\mu''(f)], \tag{13}$$

where, for $Q \gg 1$,

$$v_S^2 \approx \frac{\mu'}{\rho}, \quad v_P^2 \approx \frac{K' + \frac{4}{3}\mu'}{\rho}. \tag{14}$$

If anelasticity is entirely due to energy loss at shear deformation ($K'' = 0$), which is a widely adopted postulate and also used in the present paper, then we arrive at Eq. (5a). It is seen from Eq. (13) that proportionality of $Q_S$ and $Q_P$ exists as long as the velocity dispersion remains negligible. Even if $K''(f) \neq 0$ but is small relative to $\mu''$ or varying with frequency in a similar way, proportionality of $Q_S$ and $Q_P$ may still be assumed a good approximation.

*Seismic source spectra*

The assumption of proportionality of $\phi_P$ and $\phi_S$ certainly needs careful and critical consideration. In a homogeneous elastic medium the far-field displacement $u(r, t)$ of a seismic point source with moment function $M_0(\tau)$ may be written in terms of radial ($P$) and tangential ($S$) displacement components:

$$u^P = \frac{1}{4\pi\rho}\frac{dM_0(\tau)}{d\tau} R_P(\vartheta, \lambda)\, G_P(\Delta), \tag{15a}$$

$$u^S = \frac{1}{4\pi\rho}\frac{dM_0(\tau)}{d\tau} R_S(\vartheta, \lambda)\, G_S(\Delta). \tag{15b}$$

From Eq. (15a and b) it is evident that for a point source $u^S$ and $u^P$, and therefore also the respective source spectra $\phi_S$ and $\phi_P$, are proportional, with $R_S/R_P$ as the factor of proportionality. In our notation the radiation functions of a double couple point source are: for $P$

$$\text{(radial)} \qquad R_P(\vartheta, \lambda) = \frac{1}{v_P^3}\sin 2\vartheta \cos\lambda,$$

for $S$

$$\text{meridional} \qquad R_{Sm}(\vartheta, \lambda) = \frac{1}{v_S^3}\cos 2\vartheta \cos\lambda,$$

$$\text{(lateral)} \qquad R_{Sl}(\vartheta, \lambda) = -\frac{1}{v_S^3}\cos\vartheta \sin\lambda, \tag{16}$$

where $\vartheta$ and $\lambda$ are co-latitude and longitude on the focal sphere with respect to the fault plane and the slip vector. As an angular average one would expect to find $R_S/R_P = g \approx m$ to be of the order of $v_P^3/v_S^3 \approx 5$. Extreme

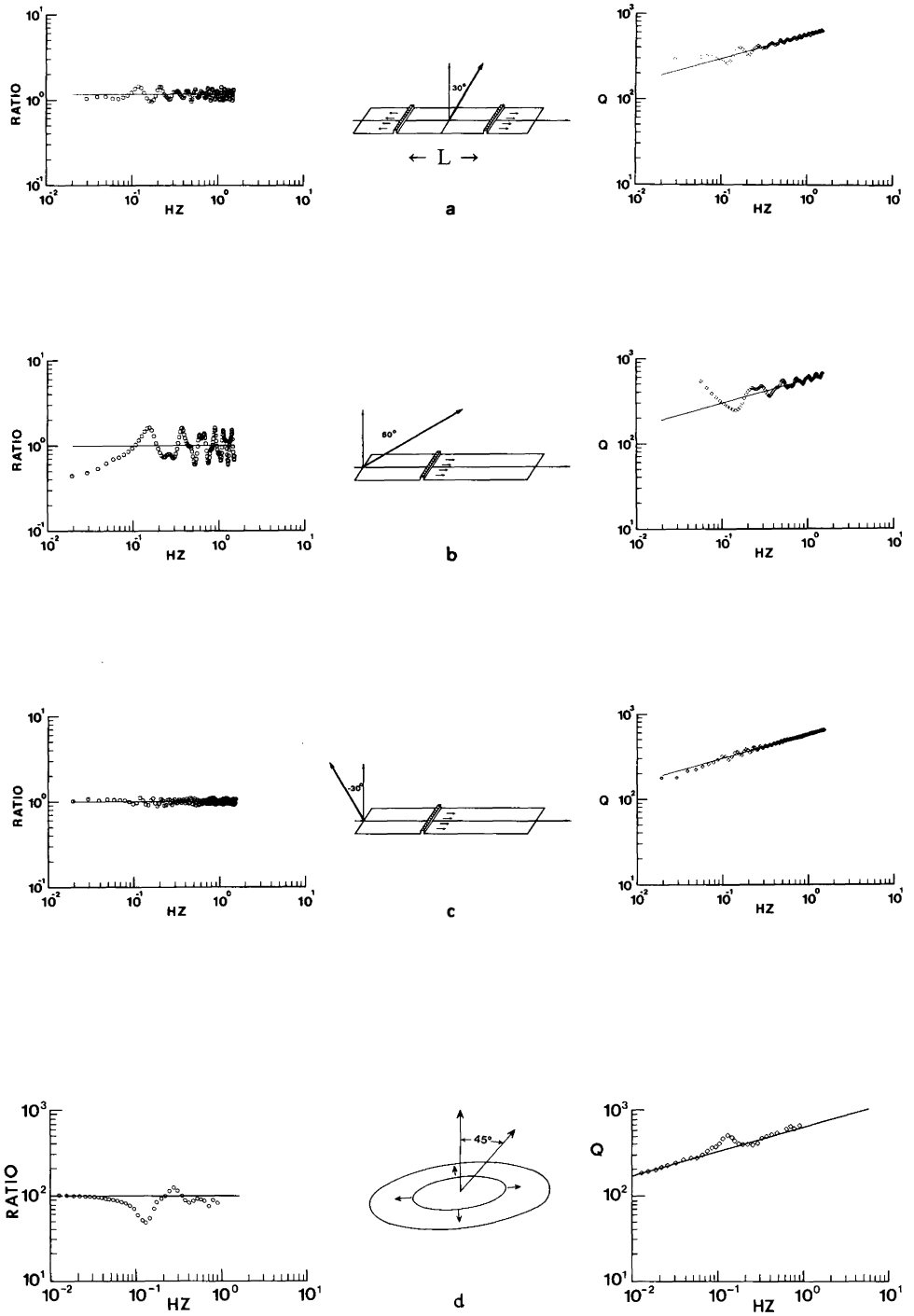


**Fig. 1.** Synthetic $S/P$-spectral ratios (*left*) and $Q$-spectra (*right*) for finite source models and different radiation angles (*middle*). *Straight lines* in the spectra correspond to a respective point source. **a–c**: Haskell type dislocation models **d**: Madariaga stress relaxation model. In the synthetic $Q$-spectra, absorption according to a power law in $Q(\alpha=0.276)$ is assumed

values are to be expected near nodal planes for $\vartheta \approx 0$, $\pi/4$, $\pi/2$ and $\lambda \approx 0$, $\pi/2$. The question is whether the proportionality of $\phi_S$ and $\phi_P$ is also a justified assumption for real earthquakes with an extended source. If we consider the corner frequencies $f^*(P)$ and $f^*(S)$ as representative quantities of the source spectra of $P$ and $S$, respectively, it turns out that the information on $f^*(P)/f^*(S)$ found in literature is controversial. Following the critical review recently published by Hanks (1981), it is found that $f^*(P)/f^*(S) > 1$ in the majority of observational cases. However, some near-source observations in low-loss material show $f^*(P)/f^*(S) \lesssim 1$. Hanks concluded from numerical estimates that different absorption of $P$- and $S$-waves may account for some of the difference of $f^*(P)$ and $f^*(S)$ but not for all. This is also not to be expected for a source of finite dimensions and finite rupture velocity.

In order to gain some feeling for the possible influence of finiteness of the source on $\phi_S/\phi_P$ in the frequency band under consideration, we have applied two different types of source models to produce synthetic source spectra.

A: One-dimensional unilateral and bilateral dislocation models of Haskell type with rupture propagation along an elongated rectangular fault of $L = 50$ km. Rupture velocities $v_r = 0.9 v_S$ and $v_r = 0.65 v_S$ were used with

**Table 1.** List of earthquakes analysed

| No. | Region name | Date | Origin time h:m:s | Coordinates: latitude $\varphi°$ | longitude $\lambda°$ | $\Delta$ degrees | Depth km | Magnitude |
|---|---|---|---|---|---|---|---|---|
| 1 | Oaxaca-Mexico | 29.11.78 | 19:52:53 | 17.0N | 96.0W | 87.9 | 49 | $Ms=7.8$ |
| 2 | St. Elias-Alaska | 28.02.79 | 21:27:08 | 60.6N | 141.6W | 68.6 | 25 | $Mb=6.8$ |
| 3 | Okinawa | 12.06.78 | 08:14:27 | 41.0N | 142.0E | 79.8 | 40 | $Ms=7.5$ |
| 4 | Alaska | 13.02.79 | 05:34:26 | 55.5N | 157.2W | 74.8 | 24 | $Ms=6.7$ |
| 5 | Mexico | 14.03.79 | 11:07:19 | 17.8N | 101.3W | 90.3 | 59 | $Ms=7.5$ |
| 6 | N. Atlantic | 22.04.79 | 09:50:18 | 33.0N | 39.7W | 40.8 | 33 | $Mb=5.7$ |
| 7 | Kodiak-Alaska | 20.05.79 | 08:14 | 56.7N | 156.7W | 73.5 | 72 | $Ms=6.7$ |
| 8 | Tibet | 20.05.79 | 22:59:16 | 32.0N | 79.0E | 52.4 | 31 | $Ms=5.5$ |
| 9 | Iran | 16.09.78 | 15:35:56 | 33.2N | 57.4E | 37.6 | 33 | $Mb=6.1$ |
| 10 | U.S.S.R. | 01.11.78 | 19:48:29 | 35.4N | 72.7E | 46.2 | 33 | $Mb=6.3$ |
| 11 | Kuriles | 06.12.78 | 14:02:03 | 44.7N | 146.4E | 78.2 | 97 | $Mb=6.5$ |
| 12 | Honshu | 07.03.78 | 02:48:46 | 32.0N | 137.4E | 85.7 | 430 | $Mb=7.0$ |
| 13 | Tibet | 18.11.77 | 05:20:11 | 33.0N | 89.0E | 58.1 | 33 | $Ms=5.9$ |
| 14 | Taiwan | 02.09.78 | 01:57:34 | 24.9N | 122.0E | 83.7 | 115 | $Mb=6.0$ |
| 15 | Colombia | 23.11.79 | 23:40:30 | 4.8N | 76.2W | 84.7 | 108 | $Mb=6.4$ |
| 16 | Japan | 18.01.81 | 18:17:24 | 38.7N | 142.8E | 82.2 | 33 | $Mb=6.2$ |
| 17 | Japan | 23.05.78 | 07:50:28 | 31.1N | 130.1E | 83.1 | 161 | $Mb=6.3$ |

$v_S=3.4$ km/s. Some typical examples of model calculations with $v_r=0.9v_S$ and arbitrary, but uniform rise-time along the fault are shown in Fig. 1a–c. Since this is only a consideration of secondary importance in the context of this paper, for details refer to Ulug (1983). The spectral ratios shown on the left of Fig. 1 are smoothed, as described in Sect. 5, and normalized by putting $R_S/R_P=1$. It is seen that the oscillations strongly depend on the radiation angle $\vartheta$ (Eq. 16). Radiation under steep angles to the rupture plane produces unimportant oscillations only (Fig. 1a and c), while comparatively large oscillations occur at low angles (Fig. 1b) due to the increasing Doppler effect. With $v_r=0.9v_S$, a rather unfavourable choice has been made in this respect. Negligible oscillations are found for a set of models with $v_r=0.65v_S$ for most radiation angles.

B: Madariaga stress relaxation models with constant rupture velocity. It may be argued that Haskell type models might lead to unrealistic results because in these models $f^*(P)\leqq f^*(S)$ (Hanks, 1981). For that reason we have also used the more sophisticated source model of Madariaga (1976). It represents a dynamic solution of the wave radiation from a circular rupture front propagating with the finite rupture velocity $v_r$. As shown by Madariaga, generally, $f^*(P)\geqq f^*(S)$. The diameter of the rupture area is chosen to be 30 km and, as in the previous models, $v_S=3.4$ km/s, $v_r=0.9v_S$. Figure 1d shows the smoothed $\phi_S/\phi_P$ ratio for a radiation angle $\vartheta=45°$. There is some disturbance in the spectral ratio slightly above the corner frequencies but very little in the lower and higher part of the spectrum.

In summary we may conclude that, despite the more or less pronounced oscillations, it is important to note that all spectral ratios follow a constant mean level throughout the frequency band which may be taken as a justification for our assumption $\phi_S/\phi_P\approx$ const.

Most of the earthquakes used in this study occurred at normal depth. No contributions of waves generated by reflections and wave conversion at the surface near the source have been taken into consideration in the models. It is to be expected that these secondary waves, if falling in the time window for spectral analysis, will create a tendency to moderate the differences between $\phi_S$ and $\phi_P$. It is a basic idea of this study that even if an individual observation might have been made under unfavourable conditions a sufficient number of cases should give, in a statistical sense, a representative picture as regards $Q(f)$.

## 4. Selection and preparation of data

For this kind of study broad-band digital seismograms with high signal/noise ratio are required. Seventeen events of $M\geqq 5.5$, recorded at the Central Seismological Observatory of the Federal Republic of Germany at Erlangen (station abbreviation GRF) at epicentral distances $40°<\Delta<90°$, were selected. Care was taken for equally good quality of $P$ and $S$ signals, i.e. for sufficient distance from nodal planes. Of the 17 earthquakes, 4 had a focal depth of more than 100 km and one was deeper than 300 km. The list of events is given in Table 1.

The frequency response of the broad-band seismometers (Wielandt and Streckeisen, 1982) is flat with respect to ground velocity from 0.05–5 Hz. The dynamic range extends to 132 dB with a resolution of 66 dB. The sampling rate is $20\,s^{-1}$. $P$-wave spectra were computed from the vertical component. $S$-wave signals were separated into $SV$ and $SH$ components. For spectral analysis, only $SH$ was used in order to eliminate $PS$ and waves converted near the receiver site.

In order to get a satisfactory spectral estimate of the signal in question, the time window $T$ was usually taken as $T\approx 3T_0$ (Abramovici, 1973), where $T_0$ is the longest period at which $P$ and $S$ still have a good signal/noise ratio. The window length had to be limited to 40–100 s to keep undesired phases like $PL$ out. Be-

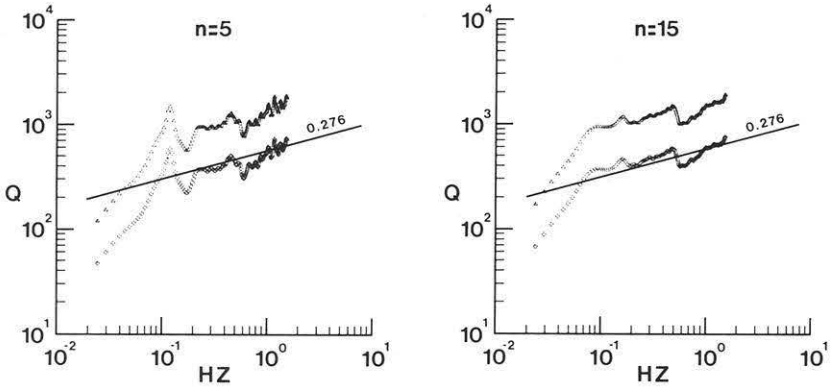


**Fig. 2.** Effect of smoothing of the spectra using the mean of $2n+1=11$ and 31 values, respectively

yond $\Delta \approx 60°$, *PcP* and *ScS* overlap with *P* and *S*, respectively. Kurita (1969) has shown that, if *PcP* and *P* or *ScS* and *S* spectra are similar, *PcP* or *ScS* respectively would modulate the *P* or *S* spectrum. Since the *PcP*/*P* amplitude ratio is less than 0.2 for $\Delta > 60°$ (Frasier and Chowdhury 1974) and *ScS*/*S* less than 0.5 for $\Delta > 70°$ (Mitchell and Helmberger, 1973), the modulation of the *P*- and *S*-spectra by *PcP* or *ScS* will not be very severe. The superposition of direct *P* and *S* with near-source surface reflections can also not be avoided for shallow foci but is, in some way, even desirable, as mentioned at the end of Sect. 3. It may, however, also cause some modulation of the source spectrum.

The choice of the shape of the time window was also subject to a comparative investigation. It turned out, however, that in practical cases the difference in the final result for a simple box car window and a cosine window, or a combination of both, was negligible. Therefore, the box car window was used.

## 5. Data analysis and results

*P*- and *S*-signal spectra were calculated by fast Fourier transformation at 1024 equidistant frequencies. For sufficient resolution at lower frequencies and since the signal to noise ratio admits only an upper signal frequency limit of 1.5 Hz, the original data were reduced to a sampling rate of 5 $s^{-1}$ corresponding to a Nyquist frequency of $f_v = 2.5$ Hz and a spectral resolution of $\Delta f \approx 0.005$ Hz.

The spectra show oscillations and break-ins caused for reasons discussed earlier (see Fig. 3). To reduce these irregularities, the raw *P*- and *S*-spectra were smoothed taking the unweighted mean of the value in question and *n* neighbouring values to both sides, i.e. of $2n+1$ values. Figure 2 shows the result of the smoothing process on $Q(f)$ for $n=5$ and $n=15$. The general trend which reflects the frequency dependence of *Q* appears more clearly after smoothing and is not modified by the procedure. The subsequent results are obtained with $n=7$.

From the smoothed signal spectra the *Q*-spectra were calculated according to Eqs. (7) and (5c). The value of *m* was determined by inserting a standard $t^*$ into Eq. (8). The full procedure is exemplified for the Kodiak-Alaska earthquake of 20 May 1979. Figure 3 shows the time functions of *P*, *S* and noise (some minutes before the *P*-onset), their raw and smoothed spectra and $Q_P(f)$ and $Q_S(f)$ in the frequency range 0.06–1.5 Hz. As a representative collection of the results obtained, the *Q*-spectra of 9 of the 17 earthquakes investigated are shown in Fig. 4. The mean of 15 *Q*-spectra, scaled at $f=1$ Hz (thick line), is given in Fig. 5, together with the standard deviation (dotted area) and two model curves. Although the spectra vary considerably in detail, they all have in common a generally increasing trend of *Q* with frequency, which may be expressed by a power law represented as a best fit straight line in the figures on bi-logarithmic scale. In Fig. 6 the $\alpha$-values of all 17 events are plotted with

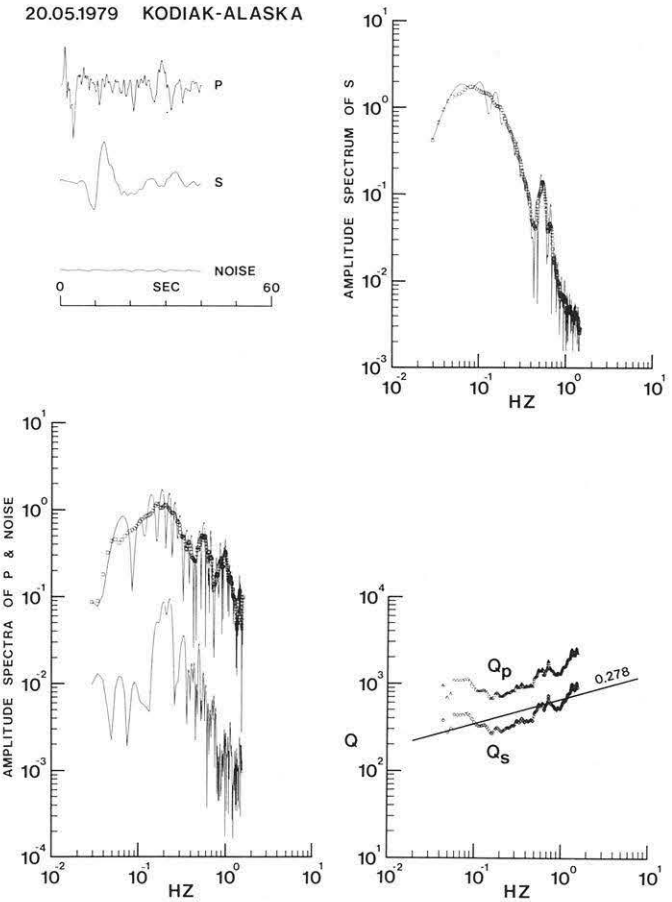


**Fig. 3.** Example of the numerical data treatment. *P*- and *S*-signal time functions, *P*, *S* and noise ground displacement Fourier spectra; $Q_P$ and $Q_S$ spectra of the earthquake of 20.05.1979 at Kodiak-Alaska, $Ms=6.7$

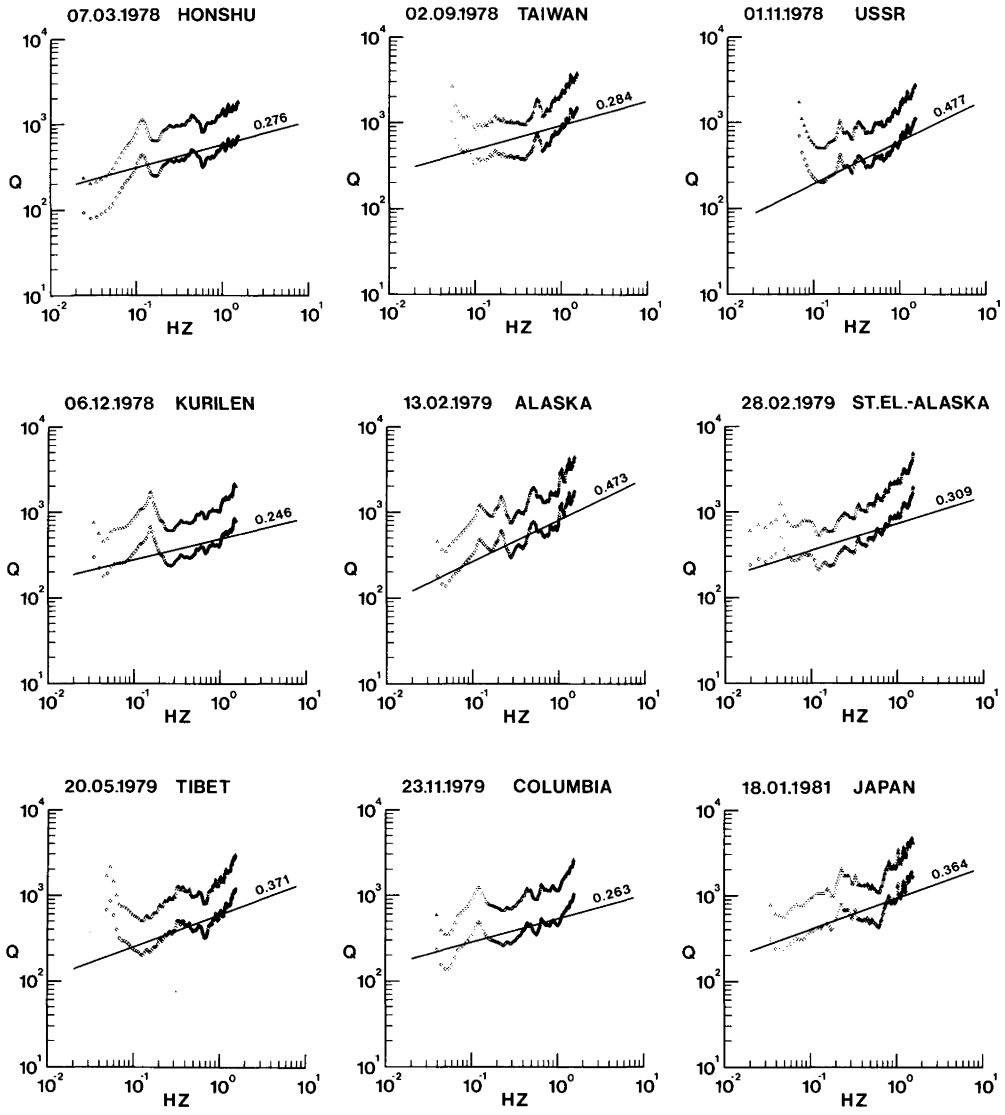


**Fig. 4.** $\bar{Q}(f)$ for $P$ (*upper curve*)- and $S$ (*lower curve*)-signals along the ray path for 9 of 17 events. Focal data are given in Table 1

rather conservative error bars versus epicentral distance. It may be concluded that $\alpha$-values range from 0.25–0.6 with some tendency to increase with decreasing distance. Since signals at shorther distances have travelled relatively longer in the asthenosphere than those which penetrated very deep in the mantle, the data may indicate that absorption in the asthenosphere is represented by higher $\alpha$-values.

In quite a number of cases, as seen from Figs. 4 and 5, a simple power law fails to describe properly the increasing slope above 1 Hz. As an alternative approach we have, therefore, attempted to fit the spectra by the high frequency end of an absorption band model with frequency independent relaxation density, as proposed by Liu et al. (1976) and applied, e.g. by Sipkin and Jordan (1979) and by Lundquist and Cormier (1980). The model curve $b$ was calculated according to

$$Q(f)=Q_B\frac{\pi}{2}\left\{\tan^{-1}\left[\frac{2\pi f(\tau_M-\tau_m)}{1+4\pi^2 f^2\tau_M\tau_m}\right]\right\}^{-1} \tag{17}$$

(Kanamori and Anderson, 1977), where $Q_B$ is the value in the absorption band and $\tau_M$ and $\tau_m$ are the upper and the lower cut-off relaxation times.

From fits of the individual $Q$-spectra with this model we obtained $\tau_m=0.33\pm0.18$ s with no significant dependence on the epicentral distance. The spectral mean in Fig. 5 is fitted with $\tau_m=0.4$ s.

## 6. Significance of the results

Before speculating on further features of the $Q$-spectra it is necessary to carefully examine factors which might have influenced the results obtained. For this purpose synthetic or semi-synthetic seismograms were used and manipulated with artificial disturbances.

Concerning the effect of the finiteness of the source on the $Q$-spectra, we make use of the model calculations of Sect. 3. On the right of Fig. 1 synthetic $Q$-spectra are shown corresponding to the respective source spectra ratio to the left. It has been presumed that anelastic absorption on the way from the source to

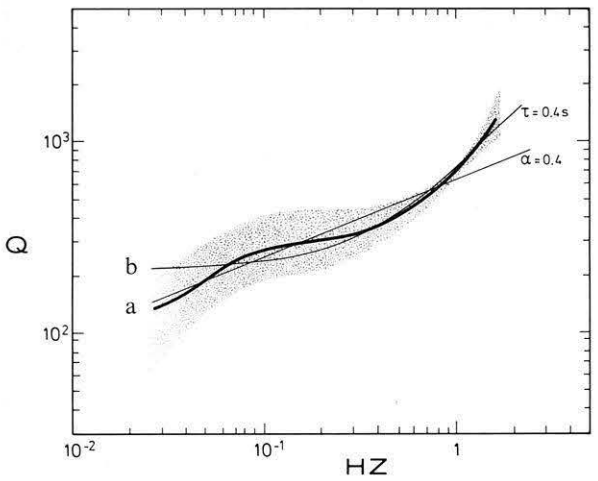


**Fig. 5.** Mean of 15 $Q$-spectra scaled at 1 Hz (*thick line*) and range of standard deviations (*dotted area*). Power law fit with $Q \approx f^{0.4}$ (a) and, alternatively, fit by a constant-$Q$ absorption band model with cut-off relaxation time $\tau_m = 0.4$ s (b)

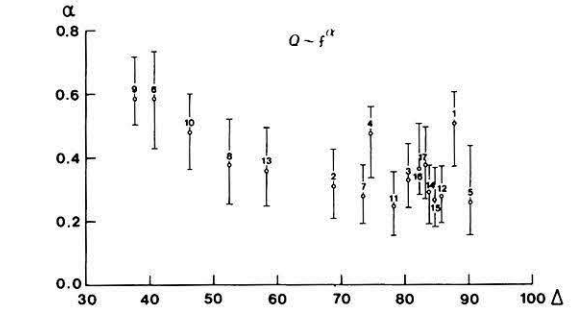


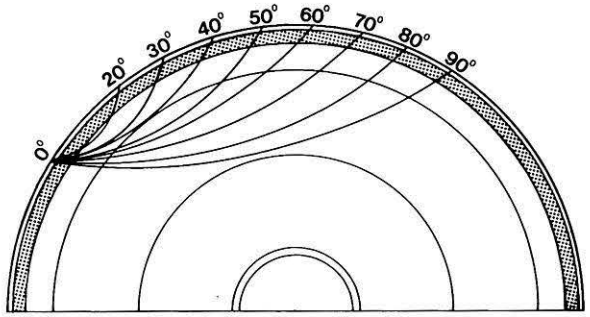

**Fig. 6.** $\alpha$-values (with error bars) of $Q(f) \approx f^{\alpha}$ for all events analysed as function of epicentral distance $\Delta$ (degrees) and the corresponding mantle ray paths

the station follows a power law $Q \sim f^{\alpha}$ with $\alpha = 0.276$. The $Q$-spectrum for an ideal source ($\phi_S \sim \phi_P$) would then be the straight line shown on all diagrams. The case 1c follows the true $Q$-spectrum very closely and 1a and d sufficiently closely. In the unfavourable case 1b we see, in particular at the low frequency end, considerable deviations but still $Q(f)$ follows the straight line in its general trend. The low frequency behaviour and some irregulatities of $Q(f)$ in the spectra of Fig. 4 might be explained by seismic source effects.

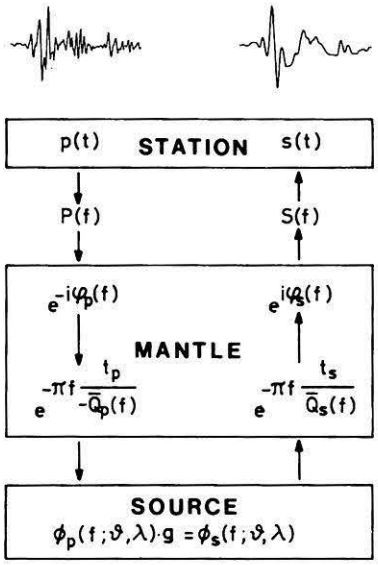


**Fig. 7.** Scheme for synthesizing an $S$-signal corresponding to an observed $P$-signal for a given $Q(f)$ model

The influence of other factors has been studied by means of a pair of semi-synthetic seismograms which are connected by an ideal power law absorption. To be most realistic we started from an actual $P$-seismogram and its Fourier transform. By inverse application of the absorption operator of an idealized anelastic mantle, the $P$-source spectrum $\phi_P$ was obtained. Assuming proportionality of $\phi_P$ and $\phi_S$, the corresponding forward operation was executed to obtain the $S$-time function corresponding to the starting $P$-signal. As seen from the scheme in Fig. 7, the process takes into account an amplitude attenuation factor, $\exp[-\pi f t/\bar{Q}(f)]$, as well as absorption linked phase shift, $\varphi(f, t)$. Absorption was assumed to follow $\bar{Q}_P(f) = Af^{\alpha}$ and $\bar{Q}_S(f) = Bf^{\alpha}$, with $A = 1{,}345$, $B = 565$ and $\alpha = 0.276$. The parameters $g \approx m$, $t_P$, $t_S$ were taken from the actual event to which the $P$-signal belonged.

The phase shift, $\varphi(f, t)$, is obtained from the approximate dispersion law for weak frequency dependence (Futterman, 1962; Kanamori and Anderson, 1977)

$$\bar{c}(f)/\bar{c}(f_0) \approx 1 + \frac{1}{\pi \bar{Q}(f)} \ln(f/f_0), \tag{18}$$

where $\bar{c}(f)$ is the mean phase velocity and $\bar{Q}(f)$ the corresponding $Q$ value along the ray. $\bar{c}(f_0)$ may be equalized with the signal velocity $v = s/t$ for $f_0 = 1$ Hz. The phase shift, $\varphi(f)$, is related to $\bar{c}(f)$ by

$$\varphi(f) = 2\pi f [t - s/\bar{c}(f)]. \tag{19}$$

The pair of $P$ and $S$ signals thus obtained was manipulated in several ways. Of course $Q(f)$, determined according to Eqs. (7) and (5c), resulted in an almost straight line with the slope of 0.276, as expected. Small deviations are attributed to numerical noise (smoothing procedure). Perhaps the most important results from these numerical experiments are those concerning the influence of artificial noise. In Fig. 8a white noise (with respect to ground velocity) is superimposed on the signal. The $Q$-spectra show a marked increase at high

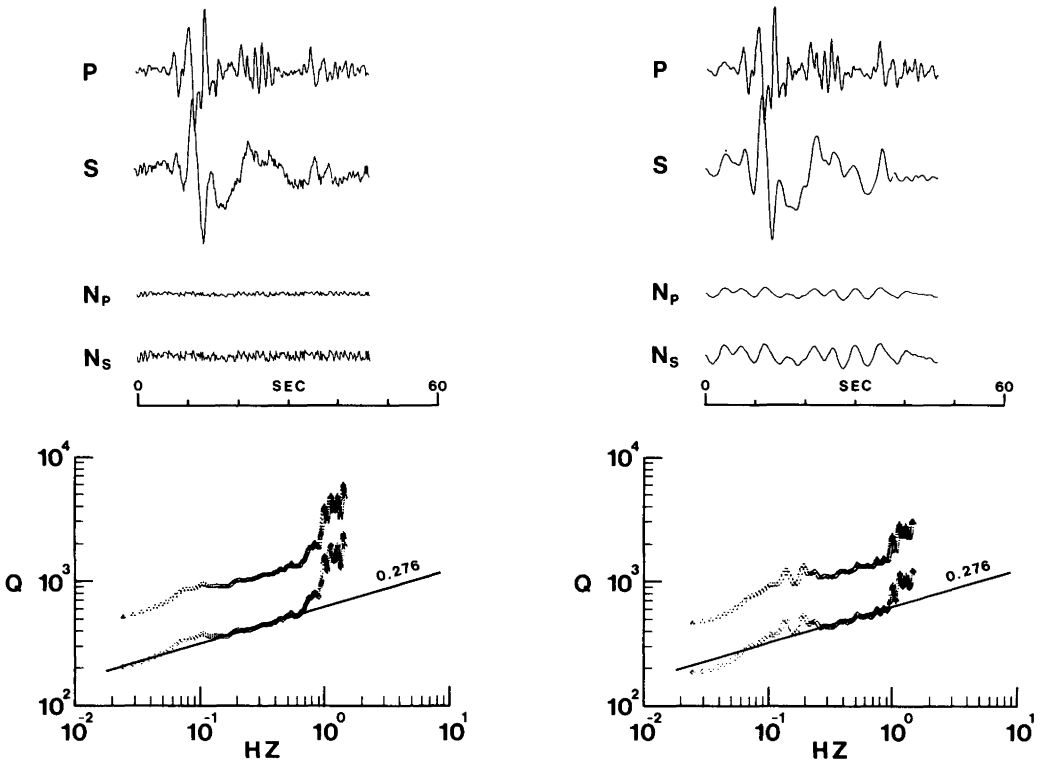


**Fig. 8.** Effect of noise, superimposed on a pair of semi-synthetic *P*- and *S*-signals, on the *Q*-spectra. *Left:* white noise; *Right:* coloured noise (central frequency 0.2 Hz)

frequencies where the signal amplitude is rapidly dropping (compare Fig. 3). However, the mean slope of 0.276 is still recognizable without difficulty. This may account, at least in part, for the rising high-frequency end of some of the *Q*-spectra in Fig. 4, and may also be of importance in judging results of other authors. In Fig. 8b the white noise is convolved with a wavelet of $T_0 = 5$ s in order to obtain "coloured" noise with a main frequency of 0.2 Hz. As expected, this tends to raise the *Q*-level in the frequency range around 0.2 Hz but $Q(f)$ still follows the slope of 0.276 quite well. From this experiment we may conclude that noise superimposed on the signal may modify the *Q*-spectrum considerably, in particular at higher frequencies, but still the general trend remains preserved.

Other experiments carried out with our semi-synthetic pair of *P*- and *S*-signals may just briefly be mentioned. As already tested with real data (Sect. 4), the shape of the time window has little influence on $Q(f)$. Variation of the length of the window by a factor of 2.5 modified $Q(f)$ only at the low-frequency end.

We may conclude this section with the following statement, valid for the frequency range considered. Several factors are capable of modifying the *Q*-spectra in detail, but no conceivable process can imitate or destroy the observed general increasing trend of $Q(f)$ which can most simply be expressed by a power law.

**Table 2.** Comparison of equivalent α-values in different investigations

| Study | α | Frequency range (Hz) |
|---|---|---|
| *Whole earth* | | |
| Anderson, Minster (1979) | 0.2–0.4 | $10^{-8}$ –$10^{-2}$ |
| *Mantle* | | |
| This study | 0.25–0.6 | 0.03 – 1.5 |
| Sipkin, Jordan (1979) | 0.35 | 0.01 – 2 |
| Der et al. (1982) | 0.15 | 0.01 – 2 |
| Sacks (1980) | 0.15–0.25 | 0.001– 0.3 |
| Clements (1982) | 0.2 –0.5 | 0.1 – 1 |
| Zschau (personal communication 1983) | 0.4 –0.6 | 0.1 – 1 |
| *Crust* | | |
| Aki (1980) | 0.6 –0.8 | 0.5 –25 |
| Mitchell (1980) | 0.3 –0.5 | 0.025– 1 |
| Singh et al. (1982) | 1.0 | 3 –25 |
| Roecker et al. (1982) | 0.5 –1.0 | 0.4 –48 |
| Thouvenot (1983) | 0.25 | 10 –25 |
| *Laboratory data* | | |
| Berckhemer et al. (1982) | 0.25 | 0.003–30 |
| Gueguen (personal communication 1982) | 0.3 | $10^{-4}$ –10 |

## 7. Discussion

*Comparison with other seismic evidence*

In this section we compare our results with those of other investigations. If only short- and long-period *Q*-values are available it is still possible to bring them into the form of a power law $Q \sim f^{\alpha}$. This has been attempted in Table 2.

Similarities in results for crust and mantle are probably just of formal character because the physical na-

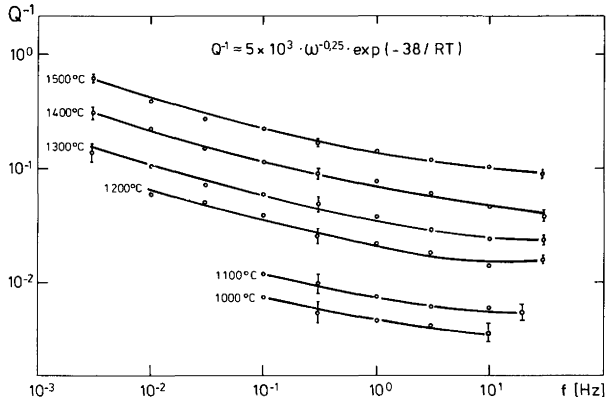


**Fig. 9.** Laboratory data on $Q^{-1}(f, T)$ for synthetic polycrystalline forsterite at shear deformation

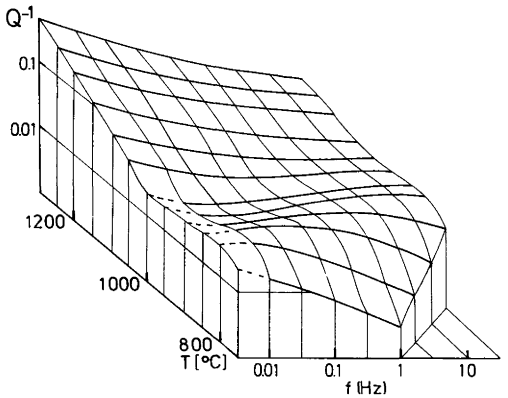


**Fig. 10.** Laboratory data on $Q^{-1}(f, T)$ for dry lherzoolite-peridotite (Balmuccia, zone of Ivrea, northern Italy) at shear deformation

ture of attenuation processes in the low-temperature, fractured and brittle crust, and in the high-temperature ductile mantle must be fundamentally different. The most specific results for the mantle, namely those of Sipkin and Jordan (1979) and ours, are in surprisingly good agreement although quite different techniques were used. The representation of the data by a power law is, however, not the interpretation given by Sipkin and Jordan. They applied relaxation band models with constant $\bar{Q}$ inside the band (see Sect. 5) and got the closest fit for a lower cut-off relaxation time $\tau_m \approx 0.4$ s. There exists, however, a gap in their data in the period range $3 < T < 15$ s which leaves some freedom for the interpretation.

As already suggested in Sect. 5, our $\bar{Q}$-spectra can probably best be represented by a power law absorption band with a slope of $0.25 < \alpha < 0.4$ and a cut-off relaxation time $0.2 < \tau_m < 0.5$ s. This model is of the type proposed recently by Anderson and Given (1982) for absorption in the mantle. Their values of $\tau_m$, however, are either considerably lower for the depth range $h < 500$ km or considerably higher for $500 < h < 2{,}300$ km. Of course it must be kept in mind that our $\bar{Q}$-values are weighted averages over the whole ray path, dominated by the absorption in the upper mantle. The effect of noise on the high-frequency end of the $\bar{Q}$-spectra, as discussed in Sect. 6, calls for care in drawing conclusions. In any case, values of $\alpha > 1$, appearing on some spectra, must be artefacts.

*Comparison with laboratory data*

Finally, let us come to the original aim of the study: the comparison of our laboratory data with $Q$ in the Earth's mantle. $Q_S^{-1}$ was measured in forced torsion oscillation experiments by the phase shift of stress and strain in the frequency range 3 mHz–30 Hz, at temperatures up to 1,500 °C and under ambient pressure of 1 bar (Berckhemer et al. 1982). The maximum shear in the sample reached values of $3 \times 10^{-5}$, which was proven to be well within the limits of linearity. Polycrystalline synthetic forsterite, natural dunite and peridotite were used as candidate materials for the upper mantle. The $Q^{-1}(f)$-spectra of dunite (Fig. 9), and similarly of polycrystalline forsterite, follow a power law with $\alpha \approx -0.25$. Apparently the whole experimental frequency range lies inside the absorption band. This is in good agreement with the seismic results, at least for $0.03 < f < 1$ Hz. The laboratory experiments with lherzolite-periodotite (about 65% olivine, 30% pyroxenes) show a similar behaviour in the experimental frequency range for $T > 1{,}200$ °C (Fig. 10). At lower temperature, however, a flat relaxation peak enters the field from the high frequency side. It appears to be the high-frequency corner of the absorption band. The slope of $Q^{-1}(f)$, however, is more gentle than $-1$ at the flank of the band, probably due to a smooth tapering-off of the relaxation density distribution. The laboratory experiments seem to reflect, at least in a qualitative way, the absorption properties of the mantle characterized by a weak power law inside the absorption band related to the so-called high-temperature background absorption (Anderson and Minster, 1979), and the high-frequency corner of the absorption band with a steeper slope.

The question is whether the increasing slope of the mantle $Q$-spectra above about 0.5 Hz (Figs. 4 and 5) may be related to the absorption band corner seen in the experimental $Q$-spectra of peridotite near 0.3 Hz at 850 °C? This is a problem of extrapolating laboratory data obtained at atmospheric pressure to asthenosphere conditions - since most of the mantle absorption takes place in the asthenosphere.

For thermally activated processes, the corner frequency $f_m \approx 1/\tau_m$ depends on temperature $T$ and pressure $p$ as $f_m = f_{m_0} \exp[(A + PV^*)/RT]$, where $A$ is the activation energy, $V^*$ the activation volume of the respective material and process and $R$ the universal gas constant. From the shift of $f_m$ with T (Fig. 10), a value of $A \approx 550$ kJ/mol (130 kcal/mol) is derived. Values of the activation volume of minerals are very scarce due to the experimental difficulties of their determination. For creep in olivine, Karato and Ogawa (1982) obtained $V^* = 16 \pm 3$ cm$^3$/mol. From dislocation recovery experiments by Kohlstedt et al. (1980), Karato (1981) derived $V^* = 19 \pm 2$ cm$^3$/mol. From creep experiments on dunite (Ross et al. 1979), Kohlstedt et al. (1980) deduced $V^* = 18$ cm$^3$/mol. Taking $V^* \approx 18$ cm$^3$/mol as a mean and taking the continental geotherm of Ito and Kennedy (1967) we shall find the experimentally observed absorption band corner under asthenosphere

conditions: for $h=150$ km ($p=50$ kbar), T = 1,050 °C at $f_m=0.7$ Hz; for $h=200$ km ($p=66$ kbar), T = 1,150 °C at $f_m=3$ Hz. Indeed, these values compare fairly well with the trend in the mantle $Q$-spectra, which suggests a causal relation. This is, however, by no means a stringent proof, because only modest variations of temperature shift $f_m$ by orders of magnitudes. $f_m$ also turns out to be strongly depth dependent and the actually observed mantle $Q$ corresponds to a weighted mean along the ray path. The latter problem was studied by Anderson and Given (1982) and by Lundquist and Cormier (1980).

## References


Abramovici, F.: Numerical application of a technique for recovering the spectrum of a time function. Geophys. J. R. Astron. Soc. **32**, 65–78, 1973

Aki, K.: Attenuation of shear waves in the lithosphere for frequencies from 0.05 to 25 Hz. Phys. Earth Planet. Inter. **21**, 50–60, 1980

Anderson, D.L., Given, J.W.: Absorption band $Q$ model for the earth. J. Geophys. Res. **87**, 3893–3904, 1982

Anderson, D.L., Hart, R.S.: Attenuation models of the earth. Phys. Earth Planet. Inter. **16**, 289–306, 1978

Anderson, D.L., Minster, J.B.: The frequency dependence of $Q$ in the earth and implications for mantle rheology and chandler wobble. Geophys. J. R. Astron. Soc. **58**, 431–440, 1979

Berckhemer, H., Auer, F., Drisler, J.: High-temperature anelasticity and elasticity of mantle peridotite. Phys. Earth Planet. Inter. **20**, 48–59, 1979

Berckhemer, H., Kampfmann, W., Aulbach, E., Schmeling, H.: Shear modulus and $Q$ of forsterite and dunite near partial melting from forced-oscillation experiments. Phys. Earth Planet. Inter. **29**, 30–41, 1982

Burdick, L.J.: $t^*$ for $S$ waves with a continental raypath. Bull. Seismol. Soc. Am. **68**, 1013–1030, 1978

Clements, J.: Intrinsic $Q$ and its frequency dependence. Phys. Earth Planet. Inter. **27**, 286–299, 1982

Der, Z.A., McElfresh, T.W., O'Donnell, A.: An investigation of the regional variations and frequency dependence of anelastic attenuation in the mantle under the United States in the 0.5–4 Hz band. Geophys. J. R. Astron. Soc. **69**, 67–99, 1982

Frasier, C.W., Chowdhury, D.K.: Effect of scattering on $PcP/P$ amplitude ratios at Lasa from 40° to 84° distance. J. Geophys. Res. **79**, 5469–5477, 1974

Futterman, W.I.: Dispersive body waves. J. Geophys. Res. **67**, 5279–5291, 1962

Hanks, T.C.: The corner frequency shift, earthquake source models, and $Q$. Bull. Seismol. Soc. Am. **71**, 597–612, 1981

Ito, K., Kennedy, G.C.: Melting and phase relations in a natural peridotite to 40 kilobars. Am. J. Sci. **265**, 519–538, 1967

Kanamori, H.: Spectrum of short-period core phases in relation to the attenuation in the mantle. J. Geophys. Res. **72**, 2181–2186, 1967

Kanamori, H., Anderson, D.L.: Importance of physical dispersion in surface wave and free oscillation problems: Review. Rev. Geophys. Space Phys. **15**, 105–112, 1977

Karato, S.: Comment on the effect of pressure on the rate of dislocation recovery in olivine, by D. L. Kohlstedt et al. J. Geophys. Res. **86**, 9319, 1981

Karato, S., Ogawa, M.: High pressure recovery of olivine: Implications for creep mechanism and creep activation volume. Phys. Earth Planet. Inter. **28**, 102–117, 1982

Kohlstedt, D.L., Nichols, H.P.K., Hornack, P.: The effect of pressure on the rate of dislocation recovery in olivine. J. Geophys. Res. **85**, 3122–3130, 1980

Kurita, T.: Spectral analysis of seismic waves, Part 1. Data windows for the analysis of transient waves. Spec. Contrib. Geophys. Inst. Kyoto Univ. **9**, 97–122, 1969

Leblanc, G.S.J.: Truncated crustal transfer functions and fine crustal structure determination. Bull. Seismol. Soc. Am. **57**, 719–733, 1967

Liu, H.-P., Anderson, D.L., Kanamori, H.: Velocity dispersion due to anelasticity; implications for seismology and mantle composition. Geophys. J. R. Astron. Soc. **47**, 41–58, 1976

Lundquist, G.M., Cormier, V.F.: Constraints on the absorption band model of $Q$. J. Geophys. Res. **85**, 5244–5256, 1980

Madariaga, R.: Dynamics of an expanding circular fault. Bull. Seismol. Soc. Am. **66**, 639–666, 1976

Mitchell, B.J.: Frequency dependence of shear wave internal friction in the continental crust of eastern North America. J. Geophys. Res. **85**, 5212–5218, 1980

Mitchell, B.J., Helmberger, D.V.: Shear velocities at the base of the mantle from observations of $S$ and $ScS$. J. Geophys. Res. **78**, 6009–6020, 1973

Okada, H., Suzuki, S., Asano, S.: Anomalous underground structure in the Matsushiro earthquake swarm area as derived from a fan shooting technique. Bull. Earthquake Res. Inst. **48**, 811–833, 1970

Roecker, S.W., Tucker, B., King, J., Hatzfeld, D.: Estimates of $Q$ in Central Asia as a function of frequency and depth using the coda of locally recorded earthquakes. Bull. Seismol. Soc. Am. 72, 129–150, 1982

Ross, J.V., Ave'Lallemant, H.C., Carter, N.L.: Activation volume for creep in the upper mantle. Science **203**, 261–263, 1979

Sacks, I.S.: $Q_s$ of the lower mantle-A body wave determination. Carnegie Institution, Ann. Rep. Dir. Department of Terrestrial Magnetism, Year Book 79, 508–512, 1980

Shimsoni, M., Ben-Menahem, A.: Computation of the divergence coefficient for seismic phases. Geophys. J. R. Astron. Soc. **21**, 285–294, 1970

Singh, K., Fried, J., Aspel, R., Brune, J.: Spectral attenuation of $SH$-wave along the Imperial Fault and a preliminary model of $Q$ in the region. Bull. Seismol. Soc. Am. **72**, 2003–2016, 1982

Sipkin, S.A., Jordan, T.H.: Frequency dependence of $Q_{ScS}$. Bull. Seismol. Soc. Am. **69**, 1055–1079, 1979

Touvenot, F.: Frequency dependence of the quality factor in the upper crust: A deep seismic sounding approach. Geophys. J. R. Astron. Soc. **73**, 427–447, 1983

Tsujiura, M.: Frequency analysis of seismic waves (1). Bull. Earthquake Res. Inst. **44**, 873–891, 1966

Ulug, A.: Frequenzabhängigkeit von $Q$ seismischer Raumwellen im Erdmantel. Ber. Inst. Meteorol. u. Geophys. Univ. Frankfurt, **49**, 1983

Wielandt, E., Streckeisen, G.: The leaf-spring seismometer: design and performance. Bull. Seismol. Soc. Am. **72**, 2349–2367, 1982


Received January 24, 1984, Revised June 6, 1984
Accepted June 8, 1984